

## Magnetic-field effects on transport in carbon nanotube junctions

L. Rosales,<sup>1</sup> M. Pacheco,<sup>1</sup> Z. Barticevic,<sup>1</sup> C. G. Rocha,<sup>2</sup> and A. Latgé<sup>3,\*</sup>

<sup>1</sup>*Departamento de Física, Universidad Técnica F. Santa María, Casilla postal 110 V, Valparaíso, Chile*

<sup>2</sup>*School of Physics, Trinity College of Dublin, Dublin, Ireland*

<sup>3</sup>*Instituto de Física, Universidade Federal Fluminense, 24210-340 Niterói, RJ, Brazil*

(Received 27 October 2006; revised manuscript received 21 February 2007; published 2 April 2007)

Here we address a theoretical study on the behavior of electronic states of heterojunctions and quantum dots based on carbon nanotubes under magnetic fields. Emphasis is put on the analysis of the local density of states, the conductance, and on the characteristic curves of current voltage. The heterostructures are modeled by joining zigzag tubes through single pentagon-heptagon pair defects, and described within a simple tight-binding calculation. The conductance is calculated using the Landauer formula in the Green-functions formalism. The theoretical approach used incorporates the atomic details of the topological defects by performing an energy relaxation via Monte Carlo calculation. The effect of a magnetic field on the conductance gap of the system is investigated and compared to those of isolated constituent tubes. It is found that the conductance gap of the studied carbon nanotube heterostructure exhibits oscillations as a function of the magnetic flux. However, unlike the pristine tubes case, they are not Aharonov-Bohm periodic oscillations.

DOI: 10.1103/PhysRevB.75.165401

PACS number(s): 73.23.-b, 72.80.Rj, 71.20.Tx

### I. INTRODUCTION

Following the numerous possibilities explored first by the semiconducting physicists, heterostructures made of carbon nanotubes (CNTs) have recently also been studied. In particular, the combination of two or more kinds of pristine tubes offers a variety of physical situation mainly due to the intrinsic feature of the carbon tubes, which exhibit electronic properties dictated by geometrical aspects.<sup>1</sup> This fact, together with quite important mechanical characteristics, make clear that CNTs may be used in different devices in science and nanotechnology.<sup>2-4</sup> The presence of topological defects can change the chirality of the CNTs. It was shown that local curvature and tube diameter do not suffer a drastic change when the defect is a pentagon-heptagon pair.<sup>5,6</sup> Actually, with this kind of defect it is possible to join two different CNTs forming a heterostructure similar to the semiconducting ones largely studied.<sup>7</sup> Metal-metal and metal-semiconducting<sup>8-12</sup> systems may be naturally formed besides the standard semiconducting composites. Of course, the electronic nature of each one of the CNT components and their symmetries will define the electronic and transport properties exhibited by the resulting heterostructures.<sup>13-18</sup> For zigzag CNTs, a change in one unity in the chiral number  $n$  [ $(n-1, 0)$  or  $(n+1, 0)$ ] leads to an electronic changing from semiconductor to metallic electronic behavior and vice versa, involving a small change in the diameter of the tubes. A similar effect may be achieved by applying a magnetic field to the carbon nanotube heterostructures (CNTH's), showing novel electronics and transport behaviors.<sup>19-23</sup> By scanning tunneling spectroscopy measurements at selected locations of CNTs it is possible to obtain a map of the electronic density of states. This technique allowed the characterization of interface states induced by the presence of defects at the junctions of two semiconducting nanotubes,<sup>24</sup> and also the determination of spatial oscillation in the electronic density of states with the period of atomic lattice.

Here we explore the gap energy modulation of nanotube heterostructures (single junctions and quantum dots) under

the action of an external magnetic field. Emphasis is put on the transport response dependence with the geometrical details of the nanostructured systems. Single junctions have been proved to be stable and in particular the stability of a  $(7,0)/(6,0)$  CNTH is verified, in the absence of magnetic fields, by calculating the total energy of the system via a numerical Monte Carlo analysis. Figure 1 shows the atomic configuration of this particular heterostructure, adopting a Tersoff empirical interatomic potential.<sup>25</sup> The topological defect (a pair of pentagon-heptagon) is highlighted in the figure with bold atomic sites (blue online). Despite of the simplicity of the potential model, it has been properly used for carbon-based materials in the determination of total and defect energy deviations, and elastic properties.<sup>26</sup> The resulting equilibrium atomic position helps us in determining the Peierl's phases<sup>1,27</sup> when considering the magnetic field since they depend on each one of the atomic positions. Monte Carlo calculations have been performed for single junctions and quantum dots heterostructures.

To investigate how uniform magnetic field changes the electronic properties of the heterostructures, we calculate local density of states (LDOS) and electrical conductance. We consider a single  $\pi$ -band tight-binding Hamiltonian and follow real-space renormalization techniques. The conductance

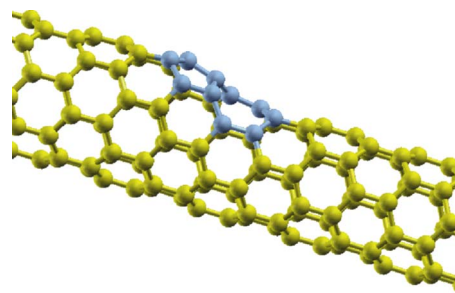


FIG. 1. (Color online) Atomic configuration of a zigzag CNTH  $[(7,0)/(6,0)]$  obtained by a Monte Carlo simulation using a semi-classical interatomic potential.

is calculated using the Landauer formula in the Green-function formalism.<sup>28</sup> We restrict our discussion to zigzag CNT junctions formed by the presence of the pair defects, as shown in Fig. 1. It is important to notice that for zigzag joining tubes the heterostructures do not present tilted angles. Therefore the external magnetic field is considered parallel to the system axis. The occurrence of the Aharonov-Bohm effect is investigated in the composed nanostructures.

## II. THEORETICAL METHOD

We restrict our present study to  $(n,0)/(n\pm 1,0)$  carbon nanotube junctions (CNTHs), and adopt a single  $\pi$ -band tight-binding Hamiltonian, taking into account a fixed value for the hopping parameter ( $\gamma_o \approx 2.75$  eV), independent of the orientation, location, and length of the bond. The systems are described in a real-space picture which allows us to incorporate the potential fluctuations at the microscopic scale. LDOS and conductance of the structures are calculated within the Green-function formalism, employing decimation procedures<sup>8,23</sup> (or, equivalently, adlayers schemes). The LDOS at site  $i$  is obtained directly from the renormalized locator  $G_{i,i}$  [ $\rho_{ii}(\omega) = -1/\pi \text{Im}(\text{Tr}(G_{ii}(\omega)))$ ]. The surface Green-functions matching formalism is used to obtain the conductance combined with an iterative calculation of transfer matrices.<sup>28</sup> Within this picture the full system is partitioned into three parts: the central one and two leads composed of two carbon nanotubes. The conductance is related to the scattering properties of the region via the Landauer formula. In the linear-response approach it can be written in terms of the Green's function of the system by<sup>29</sup>

$$\Gamma(E_F) = \frac{2e^2}{h} T(E_F), \quad (1)$$

where  $T(E_F)$  is the transmission function of an electron crossing through a central conductor, given by  $T(E_F) = \text{Tr}(\Omega_L G_c^R \Omega_R G_c^A)$ , with  $\text{Tr}$  being the matricial trace function,  $G_c^{R,A}$  the retarded and advanced Green functions corresponding to the central part of the system, and with

$$\Omega_{L,R} = i[\Sigma_{L,R}^R - \Sigma_{L,R}^A], \quad \Sigma_{L,R} = V_{c,L/R} g_{L,R} V_{L/R,c}, \quad (2)$$

describing the coupling between the central part and the right and left leads, given by the corresponding self-energies. Here the contacts are given by surface Green functions corresponding to the  $(n,0)$  and  $(n\pm 1,0)$  tubes whereas the conductor is the defective ring. All the Green functions are obtained numerically and the effects of the magnetic field are described within the Peierl's phase approximation.<sup>1</sup> In this picture phase factors named  $\Delta F_{\mathbf{R},\mathbf{R}'}$  modify the hopping energies. They depend on the local atomic neighborhood determined by the vectors  $\mathbf{R}$  and  $\mathbf{R}'$  and on the intensity of the magnetic flux  $\phi$ , which is written in terms of the quantum flux  $\phi_o = h/e$ . The matrix elements of the Hamiltonian are written as  $H_{i,j} = \gamma_o e^{ie\hbar \Delta F_{\mathbf{R},\mathbf{R}'}}$ .

One should stress that the atomic positions of the structure, including the defect region, were carefully studied using the Tersoff<sup>25</sup> relaxation process. Therefore they are incorporated into the Peierls phase calculations. In what follows,

the energies are written in terms of the hopping parameter  $\gamma_o$ , the magnetic fluxes in units of the quantum flux  $\phi_o$ , and taking into account the flux through the biggest tube of the heterostructures. The Fermi level was taken as the zero of the energies.

## III. RESULTS

Two kinds of structures are considered in this work: a single junction and a semiconductor nanotube quantum dot (CNTQD). Both are formed by the presence of the pentagon-heptagon defects. It is important to emphasize that Monte Carlo calculations were performed for both types of studied heterostructures to investigate their stability. Results for the corresponding electronic and transport properties are shown in the following subsections where we discuss the effects on a magnetic field threading the structure.

### A. Single junctions

CNTH's of type  $(n,0)/(n\pm 1,0)$  allow us to consider two types of junctions: semiconductor-metal (S/M) and semiconductor-semiconductor (S/S) configurations. Results for LDOS and conductance for a S/M [(7,0)/(6,0)] and a S/S [(8,0)/(7,0)] junctions are displayed in Fig. 2, for different magnetic-field intensities. The plotted LDOS are mean values calculated at the defective ring at which the constituent tubes change their diameter. At zero field, the LDOS of the S/M junction [(7,0)/(6,0)] exhibits a plateau close to the Fermi level, whereas the S/S [(8,0)/(7,0)] junction essentially retains the gap of the pristine (7,0). The topological defect produces the apparition of interface states in the LDOS of the S/S junction, localized close to the gap edge<sup>6,8,23,30</sup> [see Fig. 2(a)]. Both studied junctions present a wide gap in the conductance produced basically by the loss of the rotational symmetry in the defective ring.<sup>13,23</sup> The behavior of the electronic properties of the CNTH's are analyzed when the magnetic field is turned on, increasing up to one quantum flux. It is clear that, once the magnetic field is turned on, the energy gap is strongly affected, reflecting the sensitivity of the junctions to the presence of field. For magnetic fluxes equal to  $1/3$  and  $2/3$   $\phi/\phi_o$ , the LDOS of both studied junctions shows a metal-insulator-like electronic transition. However, as one can see in Fig. 2(b), those states close to the Fermi energy do not contribute to the electronic conductance of the system. This is because they are quasilocalized states and not resonant states (which was verified by means of a detailed sweeping of the LDOS in the vicinity of the junction). The presence of the topological defect produces a strong mismatch between right and left electronic wave functions, giving a null transmission probability through the junction, even in the presence of the magnetic field.

To help understand the behavior of the CNTH electronic conductance on the magnetic field, we explicitly plot in Fig. 3 the conductance gap as a function of a magnetic flux for the different studied junctions. In all cases the magnetic flux considered has been calculated using the area of the biggest tube composing the CNTH's. Actually, the smaller tubes feel a renormalized flux, scaled by a factor  $\mu = (R_n/R_{n-1})^2$ , with

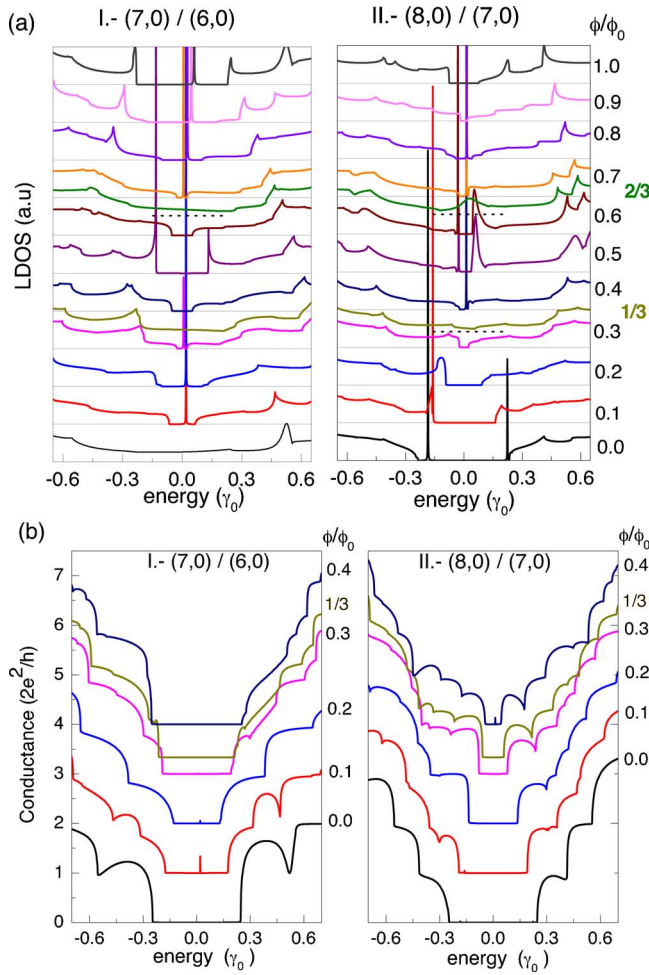


FIG. 2. (Color online) (a) LDOS at the defective ring, (b) conductance as function of energy for two types of single junctions: I, semiconductor/metal CNTH [(7,0)/(6,0)] and II, semiconducting CNTH [(8,0)/(7,0)] for different values of magnetic flux. The curves are shifted upwards for a better visualization.

$R_n$  being the  $(n,0)$  tube radius. Localized states within the gap have been ignored as they may be viewed as states of null width. A well-known result concerned to pristine straight tubes under magnetic field is that they exhibit metal-insulator-like transitions. Metallic tubes open gaps as soon as a magnetic flux starts threading it (the maximum gap occurring at a half of a quantum flux). On the other hand, a semiconducting tube closes its intrinsic gap at  $1/3$  and  $2/3$  of a quantum flux.<sup>31</sup> An Aharonov-Bohm (AB)-type effect for the gap size has been predicted and may be written in terms of the tube gap at null field.<sup>31–33</sup> The possibility of similar AB effect occurrence for the studied CNTH's has not been observed. For both CNTH's (S/S and S/M) it is found that the conductance gap of the structures is given essentially by the biggest gap of the two constituent tubes, which evolves with the magnetic flux. Similar results have been obtained for other S/S and M/S junctions.

The characteristic curves of current vs applied bias for the studied S/M and S/S junctions are shown in Fig. 4, for different magnetic-flux intensities. The current across the junction is obtained via the integration of the transmission func-

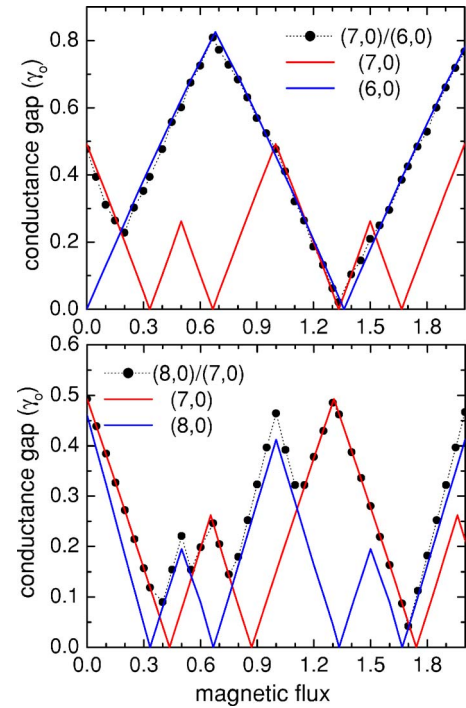


FIG. 3. (Color online) Conductance gap size as functions of the magnetic flux for the S/M [(7,0)/(6,0)] and the S/S [(8,0)/(7,0)] junctions. The conductance gaps for the pristine component tubes, composing each one of the CNTH's, are also plotted.

tion, taking into account the Fermi distribution of both leads and assuming that the total potential drop along the heterostructure (bias equal to  $V$ ) was fully restricted to the junction extension, linking both tubes.<sup>34</sup> Within this scheme, an extra potential energy was added in the diagonal term (site energy) of the tight-binding Hamiltonian. Alternatively, one may use the Keldysh formalism based on nonequilibrium Green functions<sup>35–37</sup> to calculate the transport properties in the non-linear regime. This theory is a systematic method able to

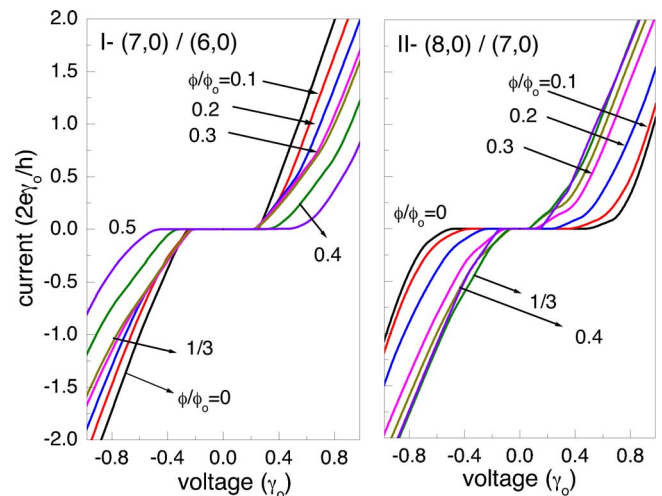


FIG. 4. (Color online) Current vs bias voltage for two types of single junctions: I, semiconductor/metal junction [(7,0)/(6,0)] and II, semiconductor/semiconductor junction [(8,0)/(7,0)] for different values of magnetic flux, from 0 to 0.5 quantum flux.

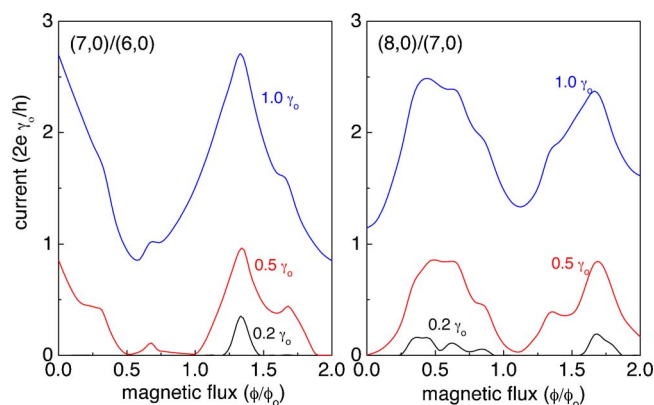


FIG. 5. (Color online) Current as a function of the magnetic flux for different applied bias. Right and left panels correspond to the  $(7,0)/(6,0)$  and  $(8,0)/(7,0)$  CNTH's, respectively.

describe the quantum transport including many-body interactions. Actually, it can be shown that both treatments are equivalent for coherent transport, i.e., in the absence of electron-phonon or electron-electron interactions.<sup>38</sup>

For zero magnetic flux the current gap size of the CNTH's is given by the mean value of the gap energies of the individual tubes. Ohmic curves are then not expected for this type of nanotube heterostructure which always involves a semiconducting part. It is easy to show that the minimum gap size is achieved for a M/S structure, being equal to  $V_{gap} = \epsilon_g/2$ , with  $\epsilon_g$  the semiconducting gap energy. Besides the band-energy shift imposed by the applied voltage, a further confinement effect is noticed when a magnetic flux threads the structure.

As is well known, the field lifts the degeneracy of the electronic states. However, differently from the case of pristine tubes, where the semiclassical electronic orbits are split leading to periodic constructive and destructive quantum interference phenomena, the CNTH's do not exhibit oscillatory current behavior. The dependence of the current on the magnetic flux for fixed voltages may prove this issue, as is shown in Fig. 5. For the current calculation, a bias is applied between the leads and therefore the corresponding chemical potentials of the two semi-infinite tubes are not aligned anymore. This fact induces strong modifications in the conductance behavior of the system as was previously analyzed<sup>18</sup> in the transport properties of biased defect-free carbon nanotubes. The AB period given by one quantum flux, observed in pristine CNT's, is destroyed. Otherwise, general features marked by peaks and valleys in the current curves are preserved for different bias intensities, although exhibiting higher current values as the bias voltage increases. Also remarkable are the differences between the current behavior of both considered CNTHs, mainly concerned to the magnetic-flux range in which they exhibit a metallic or a semiconducting character. All these points emphasize the role played by magnetic and electric fields on modifying the physical properties of nanotube structures which may be used to manipulate properly their responses and potential uses in nanoelectronics. One should also point out that a self-consistent calculation on the local charges and the energy potentials next to the topological defects would certainly provide a

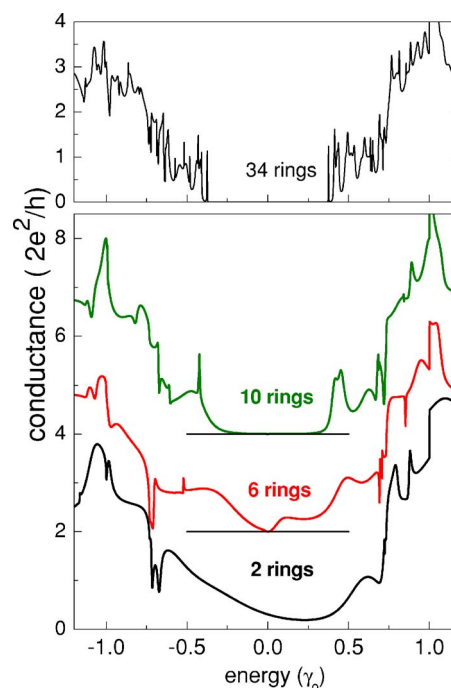


FIG. 6. (Color online) Conductance as function of the Fermi energy of  $(6,0)/(5,0)_N/(6,0)$  CNTQD's of different length:  $N=2$ , (black online),  $N=6$  (red online), and  $N=10$  (olive online). The conductance curves for  $N=6$  and  $N=10$  cases are shifted by two units of quantum conductance for a better visualization. In the upper panel  $N=34$  rings.

more realistic electronic description of the systems under study.<sup>39</sup> This is certainly important in raising the possibility of forming new nanoelectronic devices. Our preliminary studies adopting a Hubbard-like electronic Hamiltonian indicate, however, a reduction on the current response but not a dramatic change on the general trends of the simpler model.

## B. Nanotube quantum dot

Heterojunctions, such as discussed above  $(n,0)/(n-1,0)$ , are now put together to form a nanotube based quantum dot. The size of the dot is defined by the number of layers composing the internal tube, given here by the integer  $N$ ,  $(n,0)/(n\pm 1,0)_N/(n,0)$ . Results for the conductance of a  $(6,0)/(5,0)_N/(6,0)$  CNTQD in the absence of a magnetic flux are presented in Fig. 6, considering dots composed of two, six, and ten rings in the internal part, within the leads. In the upper panel, we show the conductance for a CNTQD with  $N=34$  rings. Similar to the case of single junctions, the electron-hole symmetry is lost for the quantum dot structure due to the topological defects at the interfaces of the  $(5,0)$  and  $(6,0)$  tubes. As expected, a clean gap is obtained, similar to the semiconducting gap of the  $(5,0)$  pristine CNT. The CNTQD conductance gap decreases with the size of the dot. In this example, the minimum value for the gap has been obtained for  $N=6$ , in which case zero conductance is only achieved at the Fermi energy. Applying a small gate voltage a metallic behavior for the CNTQD can be obtained. In particular, for a  $N=2$  dot (length equal to  $2a_{cc}$ ), there is a non-

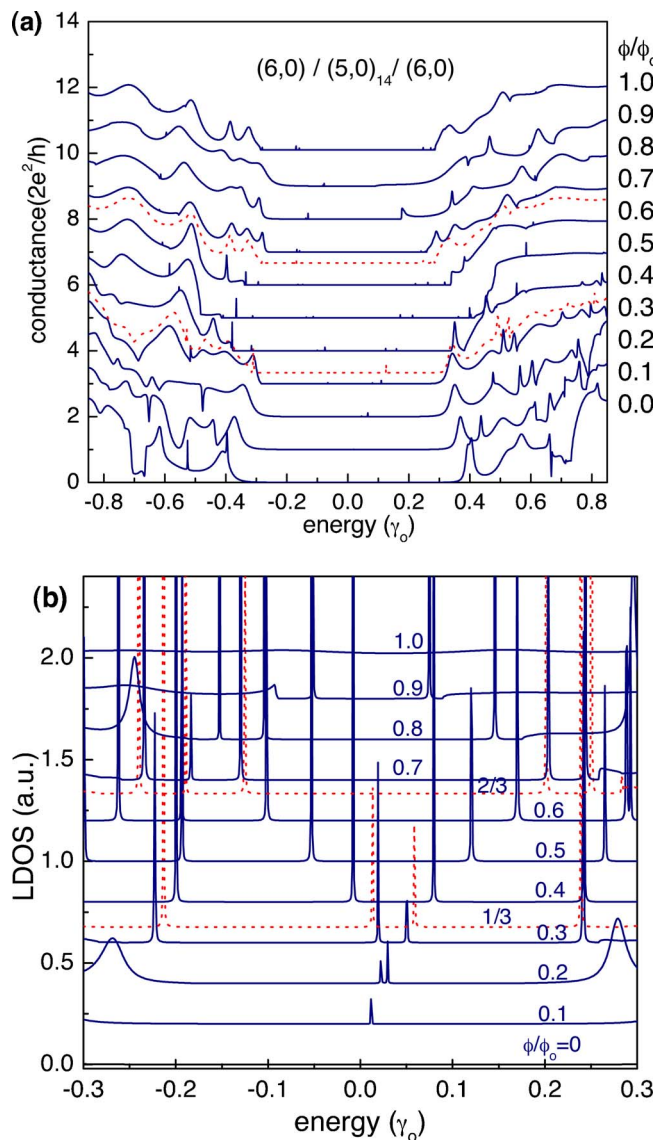


FIG. 7. (Color online) (a) Conductance behavior as a function of the energy and (b) LDOS in the energy region close to the Fermi level, for magnetic fluxes up to  $1.0\phi/\phi_0$ .

null conductance at the energy region close to the Fermi level due to the overlap between the metallic wave functions of the leads across the small dot region.

The dependence of the conductance gap on the magnetic field for a semiconducting  $(6,0)/(5,0)_{14}/(6,0)$  CNTQD is shown in Fig. 7(a). For this particular dot, a conductance gap is always present for different magnetic fluxes, in contrast to the case of a pristine  $(5,0)$  tube for which the gap closes for magnetic fluxes equal to  $1/3$  and  $2/3\phi_0$  (dashed curves in the figure). Usually, two kinds of states can be distinguished for CNTQDs: interface and resonant states. The nature of such states may be determined, for instance, by performing an accurate sweeping of the LDOS within the dot region. This region includes the interface defective rings and also a few rings within the leads.<sup>9,23</sup> Interface states are typically localized within the energy range close to the Fermi level and have a weak dependence on magnetic-field intensity. The resonant states are at energies out of the CNT gap region

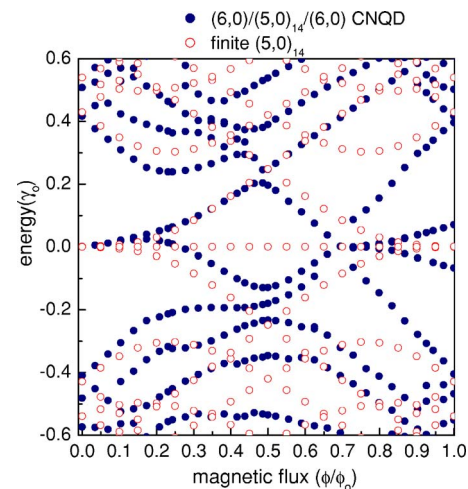


FIG. 8. (Color online) Electronic states evolution with the magnetic-flux intensities for a  $(6,0)/(5,0)_{14}/(6,0)$  CNTQD (dark circles) and for a finite  $(5,0)$  CNT, without coupled leads, formed by 14 rings (light symbols).

[ $<0.4\gamma_0$  in the present example, corresponding to the approximate gap energy at zero magnetic field, for a  $(5,0)$  tube]. For null field, this particular CNTQD structure does not exhibit localized levels in the gap region, as can be seen in the LDOS displayed in Fig. 7(b). However, as the field is turned on, the LDOS clearly shows that localized states appear close to the Fermi energy, and that they oscillate as a function of the magnetic field. The nature of the electronic states may be determined by performing low-temperature electronic transport measurements of CNTQDs with a back gate potential as reported recently.<sup>40</sup> It was shown that magnetic fields applied on such heterostructures may even induce changes in the spin configurations of the quantum dot.

The explicit dependence of the energy states on the magnetic flux is shown in Fig. 8, with full dot symbols. We have also added, for comparison, the results for a finite short  $(5,0)$  CNT, composed of 14 rings (empty dots). One should notice that in this case the results are presented as a function of the magnetic flux threading a  $(5,0)$  tube, to allow the comparison, whereas for the LDOS exhibited in Fig. 7(b) the used magnetic fluxes correspond to the bigger  $(6,0)$  tube. The finite tube energy spectrum shows states with energies near the Fermi energy corresponding to edge states whose wave functions are localized at both ends of the finite tube.<sup>41</sup> As expected, the edge state pinned at the Fermi energy, appearing for the finite CNT, is not present in the energy spectrum of the infinite quantum dot heterostructure. The magnetic-field-induced defect states of the CNTQD, shown in Fig. 7(b) as the peaked structures in the LDOS, present quite similar dependence on the magnetic field as the states of the finite tube. They may be considered as edgelike states that are lifted by the magnetic field due to the extra confinement imposed by the field. Also evident is the lack of electron-hole symmetry in the spectra of the CNTQD as the magnetic field increases, due to the presence of topological defects. Depending on the length and diameter of the dot, and also on the atomic details of the junction, different constituent tubes may be matched, forming different CNTQDs. These geometrical aspects will

dictate the presence and nature of the electronic states which, in turn, may be modulated by the magnetic flux threading the structures.

#### IV. SUMMARY

We have calculated local density of states and conductance of different heterostructures (single junctions and nanotube quantum dots) under the influence of magnetic fields. Emphasis was put on analyzing the gap modulation induced by the magnetic flux threading the structures and how the geometric details of the individual tubes composing the systems may affect the transport responses. Differently from the pristine tubes, the conductance gaps of the studied CNTHs do not exhibit AB-like periodic oscillations as a function of the magnetic flux. This lack of periodicity was also found for the characteristic curves of current vs voltage. By comparing the field dependence of the states of the dot structure with the corresponding states of the finite tube (central part of the dot) we were able to identify the nature of particular electronic states appearing in the energy range close to the Fermi level. The theoretical approach used in-

corporates the atomic details of the topological defects by performing an energy relaxation via Monte Carlo calculation. A theoretical treatment taking into account the charge fluctuations imposed by external bias is presently being studied. We believe that this kind of theoretical studies on nanotube composed systems, together with the fast development on new synthesis techniques, should help to control and modulate the physical responses of these nanostructures. Electronic transport measurements of carbon-based heterostructures with a back gate voltage may be used in order to provide insight on the nature of the localized and resonant states.

#### ACKNOWLEDGMENTS

This work was supported by the Brazilian Agencies CNPq, CAPES, FAPERJ, Instituto do Milênio, and PRONEX-CNPq-FAPERJ Grant No. 171.168-200, also by the Iniciativa Científica Milênio P02-054-F, Fondecyt 1050521 and 7060290, and Andes Foundation under the project C-14055/20, and by the Science Foundation Ireland (SFI).

\*Electronic address: latge@if.uff.br

- <sup>1</sup>R. Saito, G. Dresselhaus, and M. S. Dresselhaus, *Physical Properties of Carbon Nanotubes* (Imperial College Press, London, 1998).
- <sup>2</sup>S. J. Tans, A. Verschueren, and C. Dekker, *Nature* (London) **393**, 49 (1998).
- <sup>3</sup>W. B. Choi, D. S. Chung, J. H. Kang, H. Y. Kim, Y. W. Jin, I. T. Han, Y. H. Lee, J. E. Jung, N. S. Lee, G. S. Park, and J. M. Kim, *Appl. Phys. Lett.* **75**, 3129 (1999).
- <sup>4</sup>J. Wie, D. Wu, and H. Zhu, *Appl. Phys. Lett.* **84**, 4869 (2004).
- <sup>5</sup>B. I. Dunlap, *Phys. Rev. B* **49**, 5643 (1994).
- <sup>6</sup>J. C. Charlier, T. W. Ebbesen, and Ph. Lambin, *Phys. Rev. B* **53**, 11108 (1996).
- <sup>7</sup>T. Ando, Y. Arakama, K. Furuya, S. Komiyana, and H. Nakashima, *Mesoscopic Physics and Electronics* (Springer, New York, 1998).
- <sup>8</sup>M. S. Ferreira, T. Dargam, R. B. Muniz, and A. Latgé, *Phys. Rev. B* **62**, 16040 (2000).
- <sup>9</sup>L. Chico, V. H. Crespi, L. X. Benedict, S. G. Louie, and M. L. Cohen, *Phys. Rev. Lett.* **76**, 971 (1996).
- <sup>10</sup>M. Ouyang, J. L. Huang, C. L. Cheung, and C. M. Lieber, *Science* **291**, 97 (2001).
- <sup>11</sup>H. F. Hu, Y. B. Li, and H. B. He, *Diamond Relat. Mater.* **10**, 1818 (2001).
- <sup>12</sup>W. Fa, J. Chen, H. Liu, and J. Dong, *Phys. Rev. B* **69**, 235413 (2004).
- <sup>13</sup>L. Chico, L. X. Benedict, S. G. Louie, and M. L. Cohen, *Phys. Rev. B* **54**, 2600 (1996).
- <sup>14</sup>R. Saito, G. Dresselhaus, and M. S. Dresselhaus, *Phys. Rev. B* **53**, 2044 (1996).
- <sup>15</sup>R. Tamura and M. Tsukada, *Phys. Rev. B* **55**, 4991 (1997).
- <sup>16</sup>Z. Yao, H. Postma, L. Balents, and C. Dekker, *Nature* (London) **402**, 273 (1999).
- <sup>17</sup>L. Yang, J. Chen, H. Yang, and J. Dong, *Eur. Phys. J. B* **33**, 215 (2003).
- <sup>18</sup>A. Farajian, H. Mizuseki, and Y. Kawazoe, *Physica E* (Amsterdam) **22**, 675 (2004).
- <sup>19</sup>T. Nakanishi and T. Ando, *Physica B* **249**, 136 (1998).
- <sup>20</sup>J.-O. Lee, J.-R. Kim, J.-J. Kim, J. Kim, N. Kim, J. W. Park, and K.-H. Yoo, *Solid State Commun.* **115**, 467 (2000).
- <sup>21</sup>S. Roche, G. Dresselhaus, M. S. Dresselhaus, and R. Saito, *Phys. Rev. B* **62**, 16092 (2000).
- <sup>22</sup>A. Fujiwara, K. Tomiyama, H. Suematsu, K. Uchida, and M. Yumura, *Physica B* **298**, 541 (2001).
- <sup>23</sup>C. G. Rocha, A. Latgé, and L. Chico, *Phys. Rev. B* **72**, 085419 (2005).
- <sup>24</sup>H. Kim, J. Lee, S. J. Lee, J. Y. Park, S. J. Kahng, and Y. Kuk, *Phys. Rev. B* **71**, 235402 (2005).
- <sup>25</sup>J. Tersoff, *Phys. Rev. Lett.* **61**, 2879 (1988); *Phys. Rev. B* **37**, 6991 (1988).
- <sup>26</sup>I. Jang, S. B. Sinnott, D. Danailov, and P. Keblinski, *Nano Lett.* **4**, 109 (2004).
- <sup>27</sup>J. M. Luttinger, *Phys. Rev.* **84**, 814 (1951).
- <sup>28</sup>M. B. Nardelli, *Phys. Rev. B* **60**, 7828 (1999).
- <sup>29</sup>F. Garcia-Moliner and V. R. Velasco, *Theory of Single and Multiple Interfaces* (World Scientific, Singapore, 1992).
- <sup>30</sup>H. Liu and Y. Tao, *Nanotechnology* **16**, 619 (2005).
- <sup>31</sup>H. Ajiki and T. Ando, *J. Phys. Soc. Jpn.* **62**, 1255 (1993).
- <sup>32</sup>J. P. Lu, *Phys. Rev. Lett.* **74**, 1123 (1997).
- <sup>33</sup>T. Ando, *J. Phys. Soc. Jpn.* **74**, 777 (2005).
- <sup>34</sup>A. A. Farajian, K. Esfarjani, and Y. Kawazoe, *Phys. Rev. Lett.* **82**, 5084 (1999); A. A. Farajian, K. Esfarjani, and M. Mikami, *Phys. Rev. B* **65**, 165415 (2002).

- <sup>35</sup>L. V. Keldysh, Sov. Phys. JETP **20**, 1018 (1965).
- <sup>36</sup>C. Carioli, R. Combescot, P. Nozieres, and D. S. James, J. Phys. C **4**, 916 (1971).
- <sup>37</sup>Y. Meir and N. S. Wingreen, Phys. Rev. Lett. **68**, 2512 (1992).
- <sup>38</sup>S. Datta, *Transport in Mesoscopic Systems* (Cambridge University Press, Cambridge, UK, 1995).
- <sup>39</sup>G. Treboux, P. Lapstun, and K. Silverbrook, J. Phys. Chem. B **103**, 1971 (1999).
- <sup>40</sup>S. Sapmaz, P. J. Herrero, L. P. Kouwenhoven, and H. S. J. Zant, Semicond. Sci. Technol. **21**, S52 (2006).
- <sup>41</sup>K. Sasaki, S. Murakami, R. Saito, and Y. Kawazoe, Phys. Rev. B **71**, 195401 (2005).